Evaluation of optimum season selection for construction RSEI: A case study of ecological environment quality assessment in the Beijing-Tianjin-Hebei region from 2001 to 2020

Shaodong Huang [a, b], Yujie Li [a, b], Haowen Hu [a, b], Pengcheng Xue [a, b], Nina Xiong [a, b], Jia Wang [a, b, *]

[a] Beijing Key Laboratory of Precision Forestry, Beijing Forestry University, Beijing 100083, China
[b] Institute of GIS, RS & GPS, Beijing Forestry University, Beijing 100083, China

Abstract

Timely and objective assessment of the optimal season for the construction of remote sensing ecological index (RSEI) is of great significance for accurate and effective assessment of ecological environment quality. We manipulated RSEI in different seasons to monitor and evaluate seasonal ecological environment quality (EEQ) variations in the Beijing-Tianjin-Hebei (JJJ) region from 2001 to 2020. First, we evaluated the image quality of four seasons, and the bad observations were interpolated using the linear interpolation approach. Second, the seasonal RSEI was constructed by MODIS and its products in the years 2001, 2006, 2011, 2016, and 2020, and we compared the eigenvalues contribution rate of PC1 in different seasons. Third, we assessed the temporal and spatial variations in EEQ across the same season within distinct years. Third, Moran's I was employed to evaluate the spatial autocorrelation of EEQ, and the stability of mean and standard deviation of correlation between RSEI and four indicators of seasons was compared. Finally, the spatial distribution of Vegetation Continuous Fields (VCF) was used to compare with seasonal RSEI. The results showed that: 1) The effect of cloud/snow/ice on image quality in winter is worse than that of cloud/cloud shadow on image quality in other seasons. Additionally, the PC1 component concentrates most of the characteristics of the four indicators, especially in summer (over 71%); 2) the Moran' I in the summer of 2001, 2006, 2011, 2016, and 2020 are 0.909, 0.898, 0.917, 0.921, and 0.892, respectively, which indicated that the EEQ has a strong positive spatial correlation. 3) the correlation between the four indicators and summer RSEI showed high correlation in different years, and the standard deviation of the correlation between the four indicators and RSEI fluctuated most slightly in summer, which the std of NDVI, WET, LST, and, NDBSI were 0.005, 0.052, 0.026, and 0.017, respectively. 4) Only the RSEI in summer and the VCF show spatial distribution consistency in the long time series RSEI spatial distribution of four seasons. This study explored the spatiotemporal variations of EEQ in the JJJ region at a seasonal scale, which can provide a reference for selecting the optimum season for the ecological quality monitoring of urban agglomeration in the future.

Keywords: Optimum seasonal selection, Seasonal RSEI, JJJ region, Spatiotemporal changes, Correlation analysis

* Corresponding author. Beijing Key Laboratory of Precision Forestry, Beijing Forestry University, Beijing, 100083, China.

E-mail addresses: wangjia2009@bjfu.edu.cn (J. Wang).

1. Introduction

The status of ecological environment is inextricably linked to human survival (Yue et al., 2019). Since reforming and opening in 1978, urbanization has accelerated dramatically and Land use and Land cover (LULC) also changed significantly in China (Ji et al., 2020a), according to the National Bureau of Statistics, China's urbanization rate increased from 17.92 % to 63.89% between 1978 and 2020.(Ji et al., 2022), with China's urbanization rate expected to reach 70% by 2030.(Tian et al., 2020). Urbanization has promote the economic, social, and cultural development (Zhou et al., 2018), but it also has aggravated the pressure on ecological environment quality (EEQ) and led to a series of environmental issues (Airiken et al., 2022; Huang et al., 2021), such as biodiversity loss (McDonald et al., 2013), desertification (Zhang et al., 2018), grassland degradation (Wen et al., 2013), soil erosion (Jeong and Dorn, 2019), hydrological fluxes, and biogeochemical cycles alteration (Kalantari et al., 2017; Schneider et al., 2015), and so forth. In areas of increasing urbanization, the ecological environment has become extremely vulnerable, with a slew of ecological function degradation and eco-environmental issues (Tian et al., 2020; Zang et al., 2011). It is urgent and realistic to conduct timely, accurate, quick monitoring and quantitative assessment of the spatiotemporal changes in the eco-environment of the Beijing-Tianjin-Hebei (JJJ) region over a long time series period.

With the continuous advancement of remote sensing technology, numerous satellites with varying temporal and spatial resolutions have been launched, and due to the benefits of regular, extensive, and repetitive observations of the earth, remote sensing technology has grown in importance for eco-environmental monitoring (Huang et al., 2021; Levin et al., 2020; Turner et al., 2003). Xu (2013) proposed the remote sensing ecological index (RSEI) based on remote sensing technology, which integrated four indicators (greenness, wetness, heat, and dryness) and was used to monitor and evaluate the EEQ of Changting county in western Fujian Province. Hereafter, due to its characteristics of efficient data acquisition and objective reflection of EEQ, the RSEI has been widely used in the assessment of EEQ in various scenarios, such as in cities (Ji et al., 2020a; Maity et al., 2022; Zhang et al., 2021b), islands (Han et al., 2022; Liu et al., 2021), basins (Wu et al., 2020; Xiong et al., 2021; Zhang et al., 2022; Zhou and Liu, 2022), oases(Gao et al., 2020), plateaus (Cao et al., 2022; Sun et al., 2020), and others (Hui et al., 2021; Zhu et al., 2020).

Furthermore, MODIS and Landsat data are the most commonly used remote sensing data sources in RSEI application scenarios. However, previous research using RSEI to monitor and evaluate EEQ based on Landsat was limited to the small region level due to cloud/cloud shadow/snow contamination and the long 16-day revisit period, making it difficult to obtain all cloud-free images covering a large region at a short time. (Ji et al., 2020a). Hang et al. (2020) evaluate the impact of urbanization with RSEI based on Landsat-5 and Landsat-8 for Nanjing, Jiangsu Province. Xiong et al. (2021) used RSEI based on Landsat-5 and Landsat-8 to assess the EEQ of Erhai lake basin, Yunnan Province. Gou and Zhao (2020) used RSEI combined with Random Forest (RF) based on Landsat-8 images to monitor the EEQ of Beijing, China. Liu et al. (2021) employed RSEI based on Landsat-TM/OLI/TIRS to evaluate the spatiotemporal change of EEQ of Xiamen and Kinmen islands, China. MODIS data, on the other hand, offered a cost-effective way to monitor EEQ on a large scale and at regular intervals. (Xu et al., 2019). Some scholars applied time series RSEI based on MODIS data to evaluate the EEQ and analysis the driving factors of the JJJ urban agglomeration and China (Ji et al., 2022; Ji et al., 2020a; Ji et al., 2020b; Ji et al., 2021). Xu et al. (2019) applied

RSEI and change vector analysis (CVA) method to detect the eco-environment changes in Fujian province based on MODIS data from 2002-2017. Yang et al. (2021) calculate the RSEI based on MODIS to reveal the EEQ changes in the Yangtze River basin from 2001-2019. Liao and Jiang (2020) evaluated the spatiotemporal changes of EEQ with RSEI based on MODIS from 2000-2017 in China. Xia et al. (2022) utilized MODIS data to construct RSEI and investigate the ecological changes in Central Asia. In addition, RSEI is often calculated from a single image (Gou and Zhao, 2020; Hang et al., 2020; Liu et al., 2020; Xiong et al., 2021; Xu et al., 2018; Yuan et al., 2021), monthly images (Airiken et al., 2022; Xu et al., 2019; Yang et al., 2021), or synthesize images of vegetation growing seasonal to replace annual RSEI in the previous studies (Huang et al., 2021; Ji et al., 2022; Ji et al., 2020a).

In addition, acquiring the multi-temporal and high spatial-resolution images required for EEQ evaluation and analysis is typically time-consuming and labor-intensive (Huang et al., 2021). These issues have been resolved by the introduction of the Google Earth Engine (GEE) platform (Zhou and Liu, 2022). GEE as a free and open platform for education, research, and non-profit have widely applied, especially for research in the large regions even global scale due to its advantages of enabling parallelized processing of geospatial data (Gorelick et al., 2017). Besides, GEE hosts petabytes of over 40 years of remote sensing image, such as Landsat, MODIS, Sentinel, and Advanced Land Observing Satellite (ALOS) data (Gorelick et al., 2017; Tamiminia et al., 2020). The user-friendly frontend makes it easy to work with interactive data and develop algorithms (Mutanga and Kumar, 2019). As a result, the GEE can serve as a cloud platform for large-scale monitoring and evaluation of EEQ (Xia et al., 2022).

Till now, 272 papers on RSEI have been published both at home and abroad (including 56 international papers) (Xu and Deng, 2022). However, previous published research used RSEI to monitor and evaluate EEQ with the limitation of using a single image and composing monthly or vegetation growing images to calculate RSEI to replace the annual value, which have not explained why images from the growing season or the specific period were chosen. These studies, on the other hand, focus on EEQ inter-annual variation in a specific period while ignoring the seasonal RSEI difference. Furthermore, RSEI is composed of four indicators: greenness, humidity, dryness, and heat, and these four indicators are affected by seasonal factors such as rainfall, temperature, and vegetation growth state. All previous studies, however, have suffered from the fact that the changes in seasonal RSEI in different seasons over a long time series, as well as their correlation with the four indicators, have not been studied.

Given the issues raised above, the JJJ region was chosen as the study area to monitor and evaluate the spatiotemporal changes in EEQ in different seasons using MODIS data and the GEE platform. The goal of this study is to analysis the stability of the correlation between the four indicators and seasonal RSEI, and to examine the performance of various seasonal RSEI to the JJJ ecological quality assessments in order to determine the optimal season for assessing the ecological quality of urban metropolitan regions.

2. Materials and Methods

A workflow was established for monitoring and evaluating the changes of seasonal EEQ as well as comparing the difference of seasonal RSEI (Fig. 1). First, after removing the clouds/cloud shadow and snow/ice pixels from the images, the linear interpolation method was used to interpolate the bad observations; Second, seasonal and annual images were synthesized to calculate the RSEI for 2001,

2006, 2011, 2016 and 2020, respectively; Third, the spatiotemporal changes of EEQ were analyzed by Local indicator of spatial association (LISA) and Moran's index (Moran's I). Finally, we explored the correlation between different seasonal RSEI and the four indicators of RSEI.

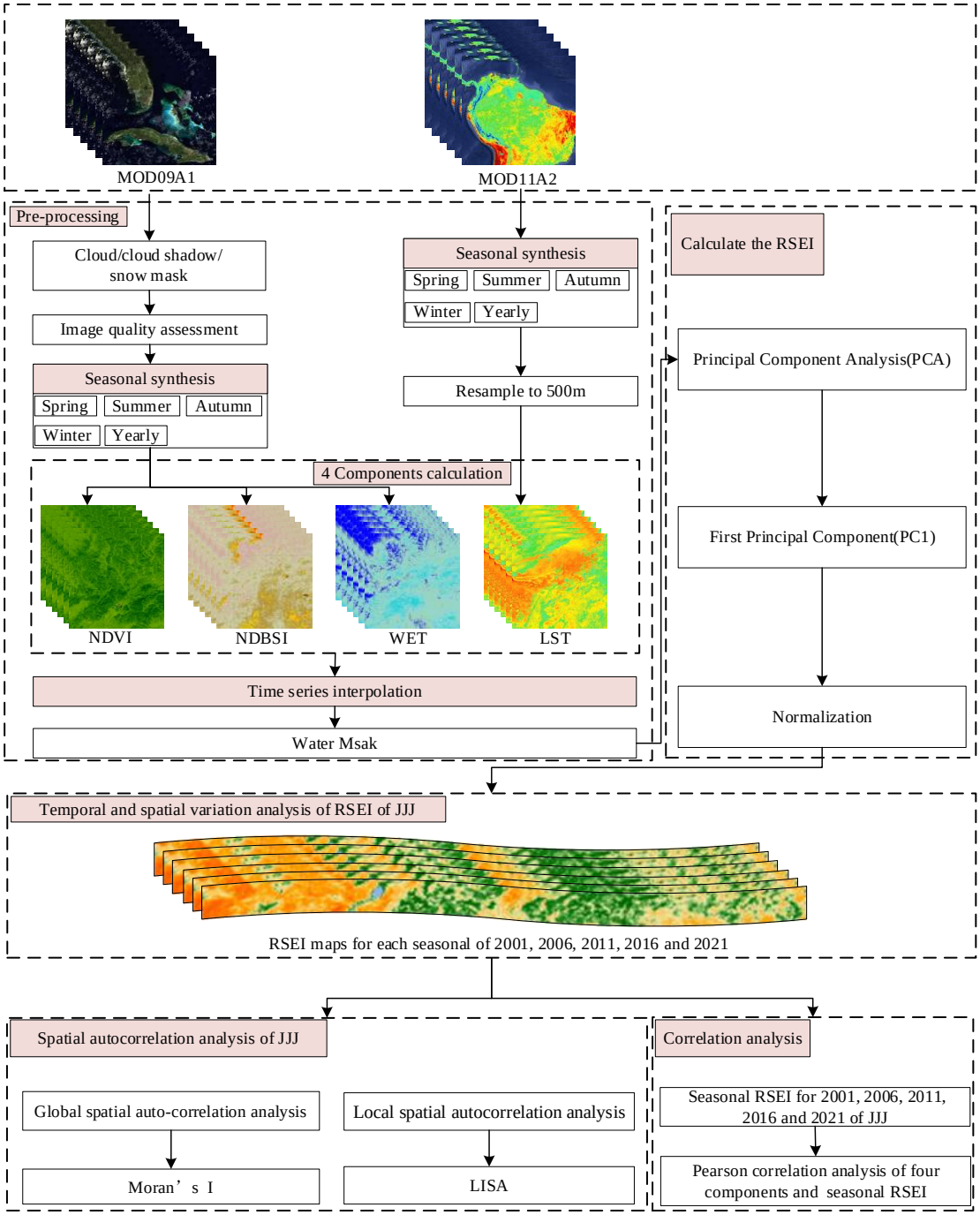

Fig. 1. Workflow of the study.

2.1 Study area

JJJ region is in northern China (36°05′ ~ 42°40′N, 113°27′ ~ 119°50′E) and covers approximately 2. 18 × 10^4 km^2 (Ji et al., 2020a) (Fig. 2). The region contains a variety of landforms. Mountains, plateaus, and basins dominate the western and northern regions, while plains dominate the eastern and southern regions (Zhang et al., 2021a). The elevation of the region is higher in the northwest than in the southeast, and the predominate land types are construction land, forest, and

grassland (Liang et al., 2022). In addition, the JJJ region was consist of the municipality directly under the central government of Beijing, Tianjin, and 11 cities in Hebei Province (Zhou et al., 2018). The coordinated development of the JJJ region is one of the three national strategies (Li et al., 2022). The JJJ region has a temperate semi-humid and semi-arid continental monsoon climate with four distinct seasons and significant annual rainfall variations (Deng et al., 2021).

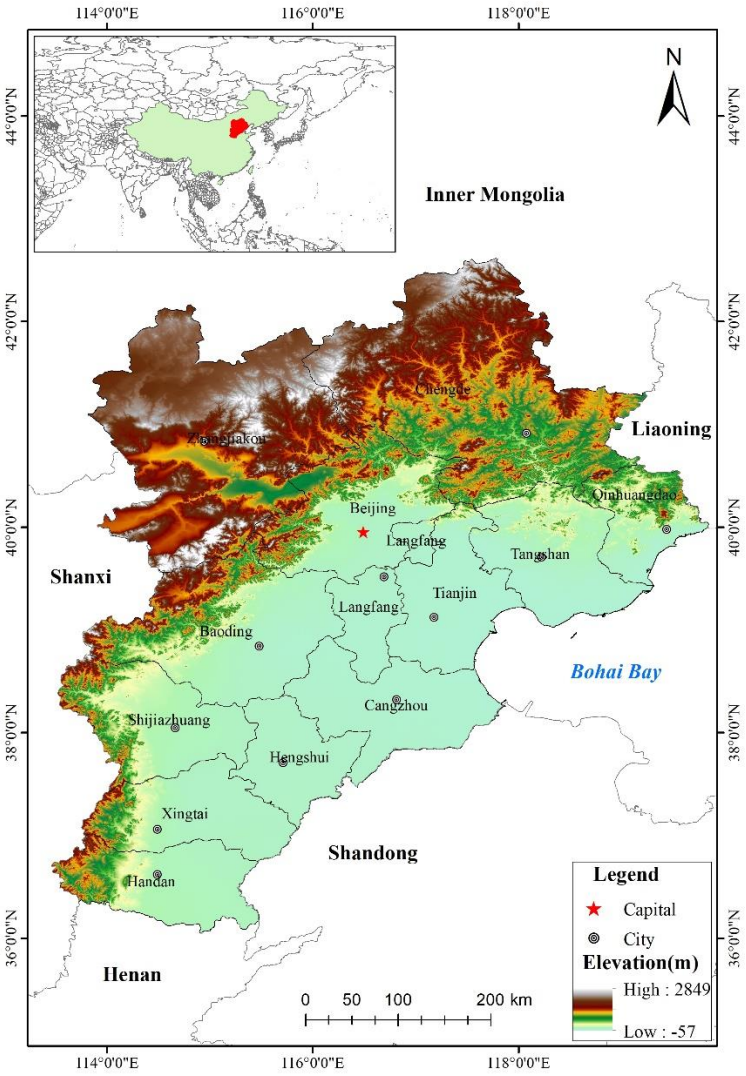

Fig. 2. Location of the Beijing-Tianjin-Hebei region.

2.2 Data and preprocessing

In this study, we employed MOD09A1 and MOD11A2 to calculate the four indicators that synthesize the RSEI. The above data were pre-processed on GEE, including corrections for atmospheric conditions such as Rayleigh scattering (Vermote et al., 2011). The MOD09A1 product provides an estimate of the surface spectral reflectance of Terra MODIS bands 1-7 at 500 m resolution (Vermote et al., 2011). The MOD11A2 product provides an average 8 days land surface temperature (LST) at 1000m resolution (Wan et al., 2015) (Table. 1). The MOD11A2 data is resampled to 500m to unify the spatial resolution of the MOD11A2 and MOD09A1(Yang et al., 2022). The images of 2001, 2006, 2011, 2016, and 2020 were synthesized based on GEE according to season (Spring: 1 Mar to 31 May; Summer: 1 Jun to 31 Aug; Autumn: 1 Sep to 30 Nov;

Winter: 1 Dec to 28 Feb of the following year) and the annual from Jan to Dec. In addition, the Vegetation Continuous Fields (VCF) product of MOD44B, which provides the surface vegetation cover estimates globally was employed to compare with the spatial distribution of the seasonal RSEI.

Table 1

Datasets catalog introduction.

Name	Resolution	Data sources	Description
MOD09A1	500m/8 days	https://lpdaac.usgs.gov/products/mod09a1v006/	A product of surface spectral reflectance of MODIS bands 1-7
MOD11A2	1000m/8 days	https://lpdaac.usgs.gov/products/mod11a2v006/	A product of land surface temperature
MOD44B	250m/ year	https://lpdaac.usgs.gov/products/mod44bv006/	A product of a sub-pixel-level representation of surface vegetation cover estimates globally

2.3 Assessment of image quality and interpolation

The quality of all MOD09A1 pixels' observations was evaluated. According to the F-mask, the bad observations of clouds/cloud shadow and snow/ice were classified as NODATA (Wang et al., 2017; Zhu and Woodcock, 2012). Since the RSEI calculation in this study was based on seasonal image synthesis, it was necessary to ensure that each composite image had at least one good observation pixel. The proportion of bad observations was counted in 13 cities in different seasons of 2001, 2006, 2011, 2016, and 2020 respectively (Fig. 3). The bad observations were mainly concentrated in winter, particularly in Chengde and Zhangjiakou. In 2016 and 2020, the number of pixels that had good observations was zero accounts for more than 16% and 20% in the winter season in Zhangjiakou respectively. To fill the bad observations, a linear interpolation method was employed for each time series based on GEE (Stöckli et al., 2005; Wang et al., 2010).

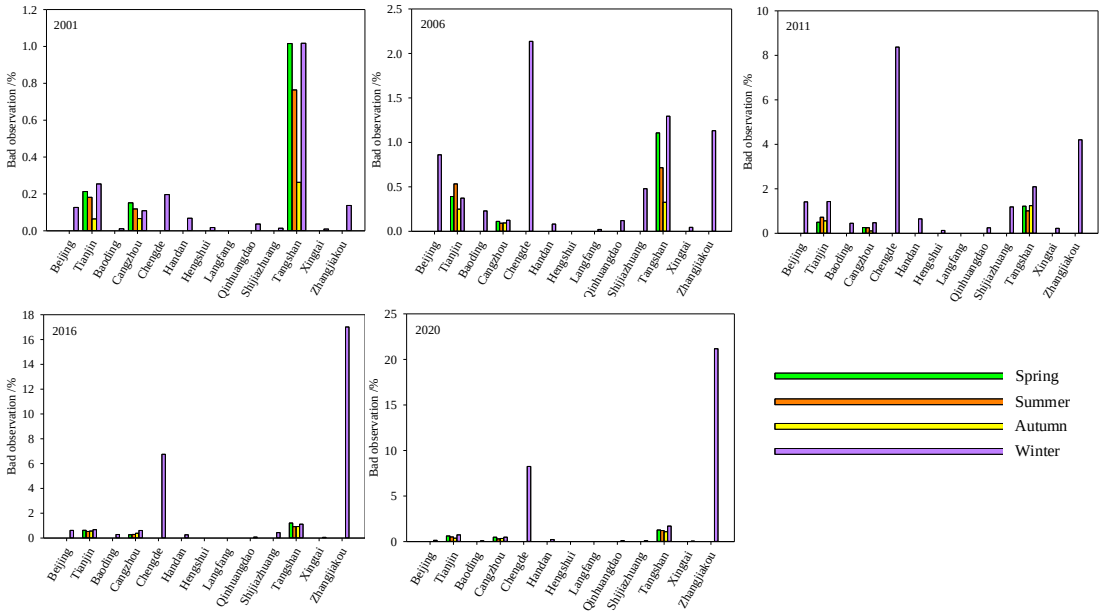

Fig. 3. Percentage of pixels with bad observations counts in the different seasons from 2001 to 2020.

2.4 Construction of remote sensing ecological indices

2.4.1 Four indicators of RSEI

RSEI was proposed by Xu and it can quickly monitor and evaluate ecological conditions solely based on remotely sensed data (Xu, 2013; Xu et al., 2018; Xu et al., 2019). The four most important indicators for the human intuitive perception of the excellent or poor quality of ecological conditions were integrated using Principal Component Analysis (PCA). (Xu, 2013). Greenness, moisture, heat, and dryness are the four indicators, which represent vegetation, soil moisture, temperature, and built lands/bare areas, respectively. (Hu and Xu, 2018; Xu et al., 2019). RSEI can be expressed as:

$$RSEI = f(Greenness, Moisture, Dryness, Heat) \quad (1)$$

Greenness denoted with NDVI can be expressed as (Rousel et al., 1973):

$$NDVI = (\rho_{NIR} - \rho_{Red})/(\rho_{NIR} + \rho_{Red}) \quad (2)$$

Wet as a component derived from Tasseled Cap Transformation (TCT) represents the moisture component of RSEI. The wet component based on MOD09A1 can be calculated as (Lobser and Cohen, 2007):

$$Wet = 0.1147\rho_{Red} + 0.2489\rho_{NIR1} + 0.2408\rho_{Blue} + 0.3132\rho_{Green} - 0.3122\rho_{NIR2} - 0.6416\rho_{SWIR1} - 0.5087\rho_{SWIR2} \quad (3)$$

NDBSI is made up of the index-based built-up index (IBI) and the soil index (SI) which represents built-up lands and bare areas according to Xu (Hu and Xu, 2018), and it can be expressed as:

$$NDBSI = (IBI + SI)/2 \quad (4)$$

$$IBI = \frac{2\rho_{SWIR1}/(\rho_{SWIR1}+\rho_{NIR})-[\rho_{NIR}/(\rho_{NIR}+\rho_{Red})+\rho_{Green}/(\rho_{Green}+\rho_{SWIR1})]}{2\rho_{SWIR1}/(\rho_{SWIR1}+\rho_{NIR})+[\rho_{NIR}/(\rho_{NIR}+\rho_{Red})+\rho_{Green}/(\rho_{Green}+\rho_{SWIR1})]} \quad (5)$$

$$SI = [(\rho_{SWIR1} + \rho_{Red}) - (\rho_{NIR} + \rho_{Blue})]/[(\rho_{SWIR1} + \rho_{Red}) + (\rho_{NIR} + \rho_{Blue})] \quad (6)$$

Heat is represented by the LST of MOD11A2 in this study. LST is an important indicator used to investigate ecological processes and climate change (Liao et al., 2022; Xu et al., 2019).

2.4.2. Integration of the four Indicators

PCA was selected to integrate the four indicators because it is a multi-dimensional data compression technique that chooses a few important variables through an orthogonal linear transformation of multiple variables. The advantage of PCA is that the weight of each indicators is determined automatically and objectively based on the character of the data and the contribution rate of each index to each principal component (Xu, 2013). The first component of PCA (PC1) explains more than 40.157% of the total variation of the dataset, especially in summer (more than 71%) (Table. 2). The contribution of each indicator to RSEI is weighted by its loading to PC1 (Xu et al., 2018). RSEI can be expressed as:

$$RSEI = PC1[f(NDVI, WET, LST, NDBSI)] \quad (7)$$

On the one hand, indicators need to be normalized to [0, 1] before PCA due to the dimensions of the four indicators is different. On the other hand, the RSEI calculated from Eq. (7) has low values for representing excellent ecological conditions and high values for negative ones (Xu et al., 2019). For high RSEI values to represent ecologically eligible and low values to represent poor ones, PCA1 needs to be subtracted from one to obtain the initial $RSEI_0$ (Xu et al., 2019).

$$RSEI_0 = 1 - [PC1[f(NDVI, WET, LST, NDBSI)]] \quad (8)$$

To facilitate the measurement and comparison of indicators, $RSEI_0$ also needs to be normalized

to [0, 1] (Xu, 2013):

$$RSEI = (RSEI_0 - RSEI_{0\_min})/(RSEI_{0\_max} - RSEI_{0\_\min}) \quad (9)$$

The RSEI calculated by Eq (9) is the final RSEI in this study, and the lower the RSEI value is, the poor the ecological condition is, while the higher the value represent the better (Xu, 2013). The RSEI is divided into 5 grades at equal intervals, representing poor, fair and moderate, good, and excellent ecological environment, respectively (Wang et al., 2016; Xu et al., 2019).

Table 2.

PCA1 of four indicators in different seasons.

Year	Index	PCA1				
		Spring	Summer	Autumn	Winter	Yearly
2001	NDVI	0.552	0.564	0.551	0.097	0.525
	WET	0.487	0.372	0.515	0.261	0.511
	NDBSI	-0.630	-0.594	-0.649	-0.533	-0.575
	LST	-0.247	-0.437	-0.013	-0.799	-0.363
	Eigenvalues	0.115	0.156	0.102	0.090	0.100
	Eigenvalues contribution rate (%)	64.335	**80.669**	56.571	46.363	54.907
2006	NDVI	0.541	0.586	0.541	0.192	0.542
	WET	0.496	0.318	0.522	0.316	0.517
	NDBSI	-0.669	-0.559	-0.640	-0.554	-0.535
	LST	-0.118	-0.493	-0.159	-0.746	-0.391
	Eigenvalues	0.102	0.163	0.100	0.073	0.093
	Eigenvalues contribution rate (%)	57.194	**78.675**	53.942	40.157	49.247
2011	NDVI	0.601	0.575	0.574	0.021	0.538
	WET	0.507	0.275	0.466	0.032	0.451
	NDBSI	-0.600	-0.567	-0.672	-0.317	-0.488
	LST	-0.120	-0.521	-0.036	-0.947	-0.519
	Eigenvalues	0.105	0.144	0.110	0.085	0.113
	Eigenvalues contribution rate (%)	57.515	**74.890**	55.173	42.818	59.426
2016	NDVI	0.613	0.586	0.600	0.287	0.559
	WET	0.481	0.315	0.486	0.544	0.394
	NDBSI	-0.625	-0.567	-0.566	-0.438	-0.500
	LST	-0.040	-0.486	-0.288	-0.656	-0.531
	Eigenvalues	0.115	0.139	0.100	0.083	0.120
	Eigenvalues contribution rate (%)	58.341	**78.255**	51.548	43.990	63.228
2020	NDVI	0.606	0.582	0.605	0.189	0.644
	WET	0.509	0.325	0.531	0.547	0.474
	NDBSI	-0.609	-0.552	-0.583	-0.177	-0.562
	LST	-0.049	-0.501	-0.106	-0.796	-0.210
	Eigenvalues	0.120	0.125	0.093	0.079	0.108
	Eigenvalues contribution rate (%)	60.707	**71.297**	50.087	45.208	55.982

2.4.3. Detection of ecological condition changes in the same season of different years

To reveal the dynamic change of EEQ in the same season of different years, the difference in

RSEI levels was calculated in 5 periods (2001 to 2006, 2006 to 2011, 2011 to 2016, 2016 to 2021, and 2001 to 2020). For each pixel in the study area, we defined the score from 1 to 5 corresponding to the five ecological condition levels from poor to excellent, respectively. The difference in EEQ score between years ranged from -5 to +5. When the score is positive (1, 2, 3, 4, 5) it indicates that the EEQ has improved; when the score is 0 represented there has no change, and while the score is negative (-1, -2, -3, -4, -5) represented the EEQ has de graded. In addition, a lower score indicates a more serious ecological degradation, whereas a higher score indicates a better ecological environment.

2.4.4. Spatial autocorrelation analysis

Moran's I and LISA are often used to analyze the spatial autocorrelation of EEQ (Jing et al., 2020; Xiong et al., 2021). Moran's I reflect the correlation between the neighbouring units (the pixels of 500m×500m) of geospatial space, and a value closer to 1, the stronger the correlation between units. Therefore, we utilized Moran's I to verify the correlation between the RSEI units in this study, which can be expressed as (Gong et al., 2014):

$$Globalmoran's\ I = \sum_{i=1}^{n}\sum_{j=1}^{m} W_{ij}(x_i - \bar{x})\left(x_j - \bar{x}\right)/S^2 \sum_{i=1}^{n}\sum_{j=1}^{m} W_{ij} \quad (10)$$

$$S^2 = \sum_{i=1}^{n}(x_i - \bar{x})^2/n \quad (11)$$

where n is the grids in this study area; i =1, 2, 3 …, n; j = 1, 2, 3 …, m. x_i is the RSEI value of the location of i; $\bar{x}$ represent the average RSEI values of all units in this study area; S^2 is the spatial units variance; W_{ij} is the weight matrix which can represent the relationship of spatial units. Moran's I values range from -1 to 1, with a value close to 1 indicating that the RSEI of spatially adjacent units is positively correlated and a value close to -1 indicating that it is negatively correlated. LISA index as an important index to analyze local spatial autocorrelation due to it can calculate the value of Moran's I at each spatial unit. Therefore it is to (Anselin, 1995). In this study, LISA was used to analyze the correlation of EEQ in each unit, the equation as follows (Gong et al., 2014; Xiong et al., 2021):

$$Localmoran's\ I = [(x_i - \bar{x})/S^2]\sum_{j=1}^{m} W_{ij}(x_i - \bar{x}) \quad (12)$$

Where positive I indicates that adjacent space units have similar values (both high or both low), whereas negative I indicates that adjacent units have large value differences.

2.4.5. Pearson's correlation analysis

For the terrestrial ecosystem, its EEQ may be determined by the four indicators of RSEI (Yuan et al., 2021), but the effects of these indicators on seasonal RSEI are unclear. In order to analyze which indicator influences EEQ in different seasons in this study area, the Pearson correlation analysis method was conducted for seasonal RSEI and the four indicators. The function can be calculated as (Ahlgren et al., 2003):

$$\rho = \sum_{i=1}^{N}(x_i - \bar{x})\,(y_i - \bar{y})/\sqrt{\sum_{i=1}^{N}(x_i - \bar{x})^2 \sum_{i=1}^{N}(y_i - \bar{y})^2} \quad (13)$$

Where ρ denotes Pearson's correlation coefficient. When ρ is close to 0, the two variables are not correlated; when ρ is close to -1 or 1, a strong correlation between the two variables.; N is the number of spatial units; x_i and y_i denote the values of variables and RSEI of its units respectively; $\bar{x}$ denotes the mean of the variables; $\bar{y}$ represents the mean value of RSEI.

3. Results

3.1 Spatiotemporal changes of seasonal EEQ

Most the four indicators' characteristic information is concentrated on PC1. However, the contribution rate varies by season, with summer having a significantly higher eigenvalues contribution rate (more than 71%) than the other three seasons (Table. 2). This may be explained by Xu (2013), who states that vegetation greenness is a key factor for RSEI (Xu and Deng, 2022), therefore the eigenvalues contribution rate of PC1 of vegetation growing season is higher.

The variation of the seasonal RSEI mean values was depicted in Fig. 4. The graph showed that RSEI showed different trends in different seasons under the long time series. Therefore, different seasons to construct RSEI will lead to significant differences in the assessment of ecological quality. The RSEI in summer are 0.423, 0.480, 0.505, 0.481, and 0.509, respectively, showing a trend of rising, declining, and rising.

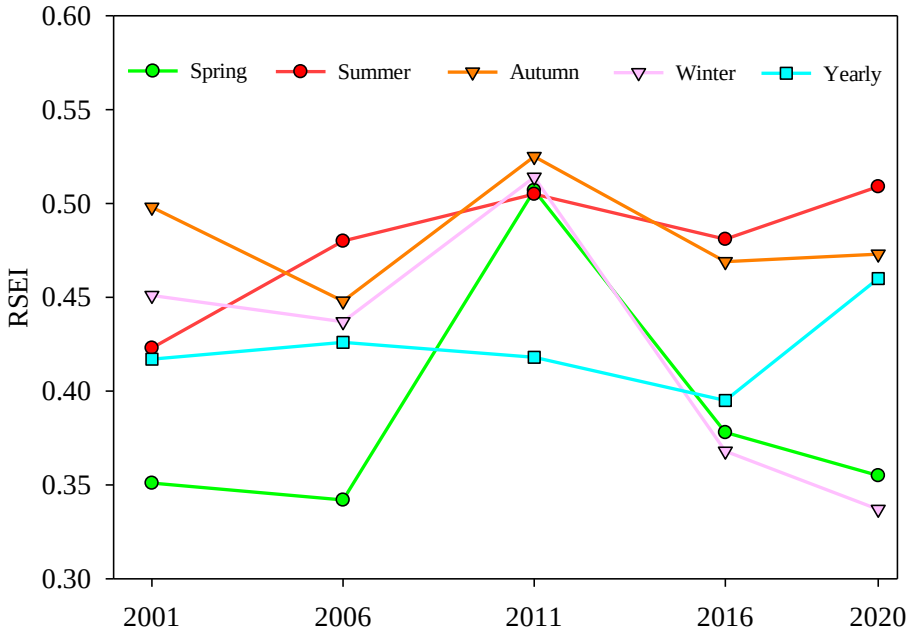

Fig. 4. The variation of the seasonal RSEI in the JJJ region from 2001 to 2020.

In addition, the spatial distribution of RSEI based on seasonal images also varies greatly (Fig. 5). Except for the southern part of the study area, the ecological quality was poor in other regions in spring (Fig. 5a, f, k, p, u), and the ecological quality was better in northeast, but worse in northwest and south in summer (Fig. 5b, g, l, q, v). In autumn, the ecological quality of northwest JJJ is poor while that of other regions is better (Fig.5c, h, m, r, w). The spatial distribution of RSEI in winter was different in terms of inter-annual variation, and the ecological quality was better in the south of JJJ region in the first three years while worse in the second two years (Fig. 5d, i, n, s, x). However, the spatial distribution of RSEI throughout the year is consistent with that in summer (Fig. 5e, j, o, t, y).

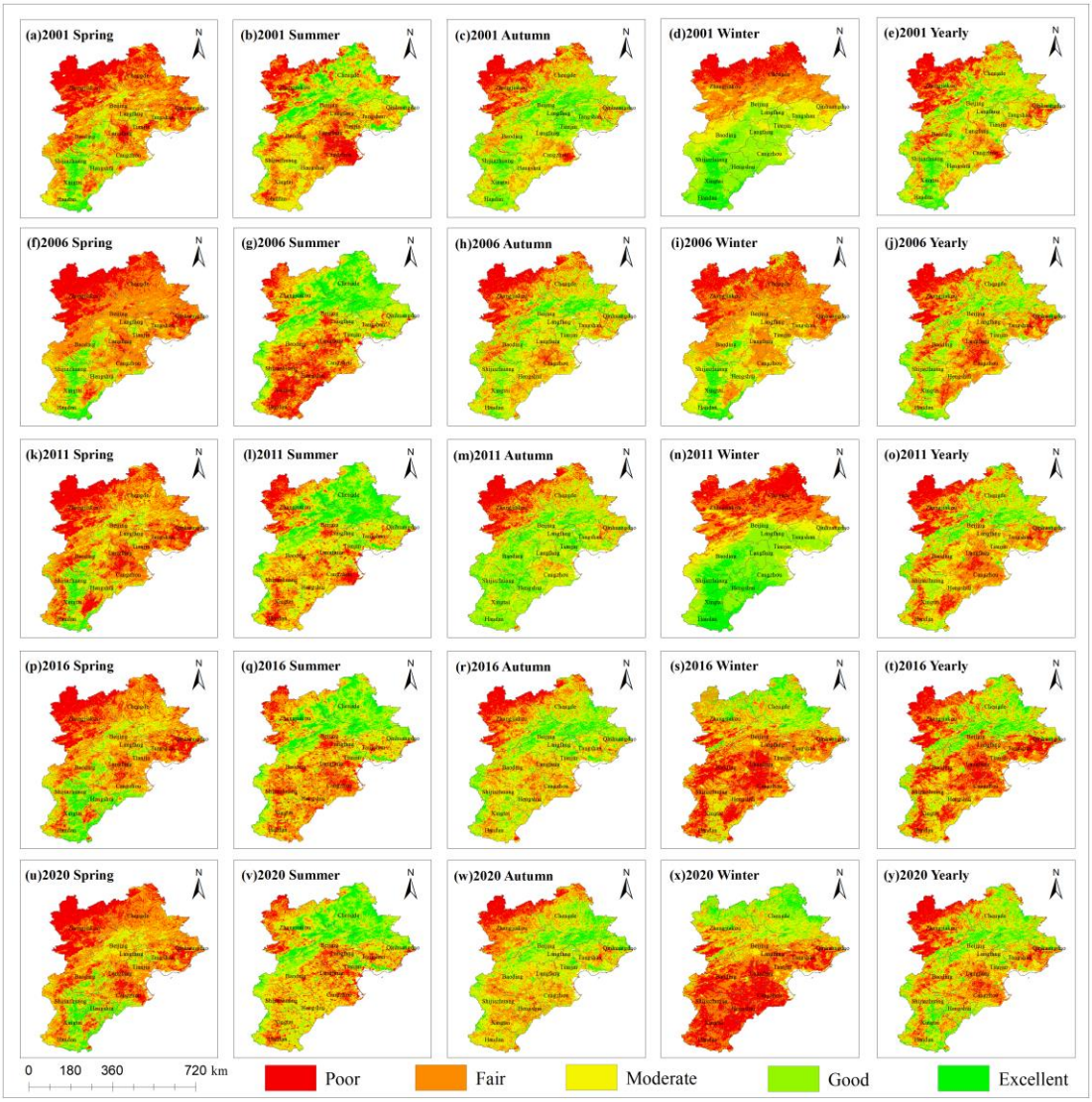

Fig. 5. Spatial-temporal distribution of EEQ of the JJJ region in different seasons from 2001 – 2020.

3.2 Dynamic change analysis of EEQ

The spatiotemporal change of EEQ in the same season of different years and scores are shown in Fig. 6 and listed in Table. 3. In fact, the scores are mainly concentrated on -1, 0, and 1. In addition, compared with the pixels with the changes, the pixels with unchanged of EEQ accounted for the largest proportion in spring (Fig. 6a, f, k, p, u), summer (Fig. 6b, g, l, q, v), autumn (Fig. 6c, h, m, r, w), and yearly (Fig. 6e, j, o, t, y). Except in winter (Fig. 6d, i, n, s, x), the proportion of pixels with scores of -4, -3, +3, or +4 does not exceed 8% respectively. It proves that despite ecological quality assessment at five-year intervals, ecological changes are not significant. No matter which season, however, the change of ecological quality will not continue to get better or worse, there is always a trend of fluctuation under a long time series. The spatiotemporal changes of EEQ in summer, for example, in the south of the study area was first degraded from 2001 to 2006 (Fig. 6b), then improved from 2006 to 2011 (Fig. 6g), and began to degraded from 2011 to 2016 (Fig. 6l), then increase again from 2016 to 2020 (Fig. 6q). However, although the ecological quality fluctuated in the past 20 years, the ecological quality of the study area showed a trend of improvement (Fig. 6v).

306 **Table 3**

307 RSEI levels change in the same seasons from 2001 to 2020.

Periods	Scores	Spring	Summer	Autumn	Winter	Yearly
		Pct/%	Pct/%	Pct/%	Pct/%	Pct/%
2001 to 2006	+4	0.00	0.80	0.00	0.00	0.00
	+3	0.06	6.44	0.21	0.12	0.09
	+2	1.14	14.27	3.69	11.25	3.04
	+1	19.69	27.45	29.20	41.03	28.03
	0	68.78	36.11	53.40	37.26	55.71
	-1	10.11	12.34	12.55	8.69	12.51
	-2	0.21	2.38	0.92	1.46	0.58
	-3	0.01	0.21	0.03	0.18	0.02
	-4	0.00	0.00	0.00	0.01	0.00
2006 to 2011	+4	0.00	0.00	0.00	0.03	0.00
	+3	0.03	0.03	0.02	0.50	0.02
	+2	0.92	1.22	0.75	2.75	0.85
	+1	16.19	17.01	11.95	11.44	18.32
	0	62.45	54.65	49.16	29.81	64.40
	-1	19.17	22.13	30.36	33.43	16.05
	-2	1.18	4.57	7.11	20.50	0.35
	-3	0.05	0.39	0.62	1.54	0.01
	-4	0.00	0.00	0.03	0.01	0.00
2011 to 2016	+4	0.00	0.00	0.04	2.19	0.00
	+3	0.03	0.12	0.80	19.79	0.04
	+2	0.35	2.11	7.31	23.31	1.33
	+1	8.95	25.30	26.64	12.88	26.49
	0	64.80	58.08	44.80	10.49	57.84
	-1	22.88	13.24	18.45	11.55	13.85
	-2	2.68	1.09	1.87	9.70	0.44
	-3	0.28	0.06	0.09	6.78	0.01
	-4	0.03	0.00	0.00	3.31	0.00
2016 to 2020	+4	0.03	0.00	0.02	0.04	0.00
	+3	0.21	0.03	0.22	0.34	0.23
	+2	1.49	0.54	2.61	3.97	9.19
	+1	21.34	11.98	20.91	20.67	53.04
	0	67.22	61.43	54.66	57.45	33.45
	-1	9.29	23.58	19.75	14.45	3.93
	-2	0.39	2.31	1.71	2.08	0.17
	-3	0.03	0.14	0.10	0.94	0.01
	-4	0.00	0.00	0.01	0.06	0.00
2001 to 2020	+4	0.04	0.11	0.02	3.30	0.01
	+3	0.56	2.04	0.87	21.47	0.41
	+2	3.29	13.49	7.45	19.54	4.39
	+1	17.62	32.25	24.32	13.26	22.30
	0	58.60	36.64	43.33	9.81	49.40
	-1	17.58	12.34	20.77	11.78	21.10
	-2	2.02	2.72	3.09	10.21	2.29
	-3	0.29	0.40	0.15	7.15	0.10

-4	0.01	0.02	0.01	3.48	0.00

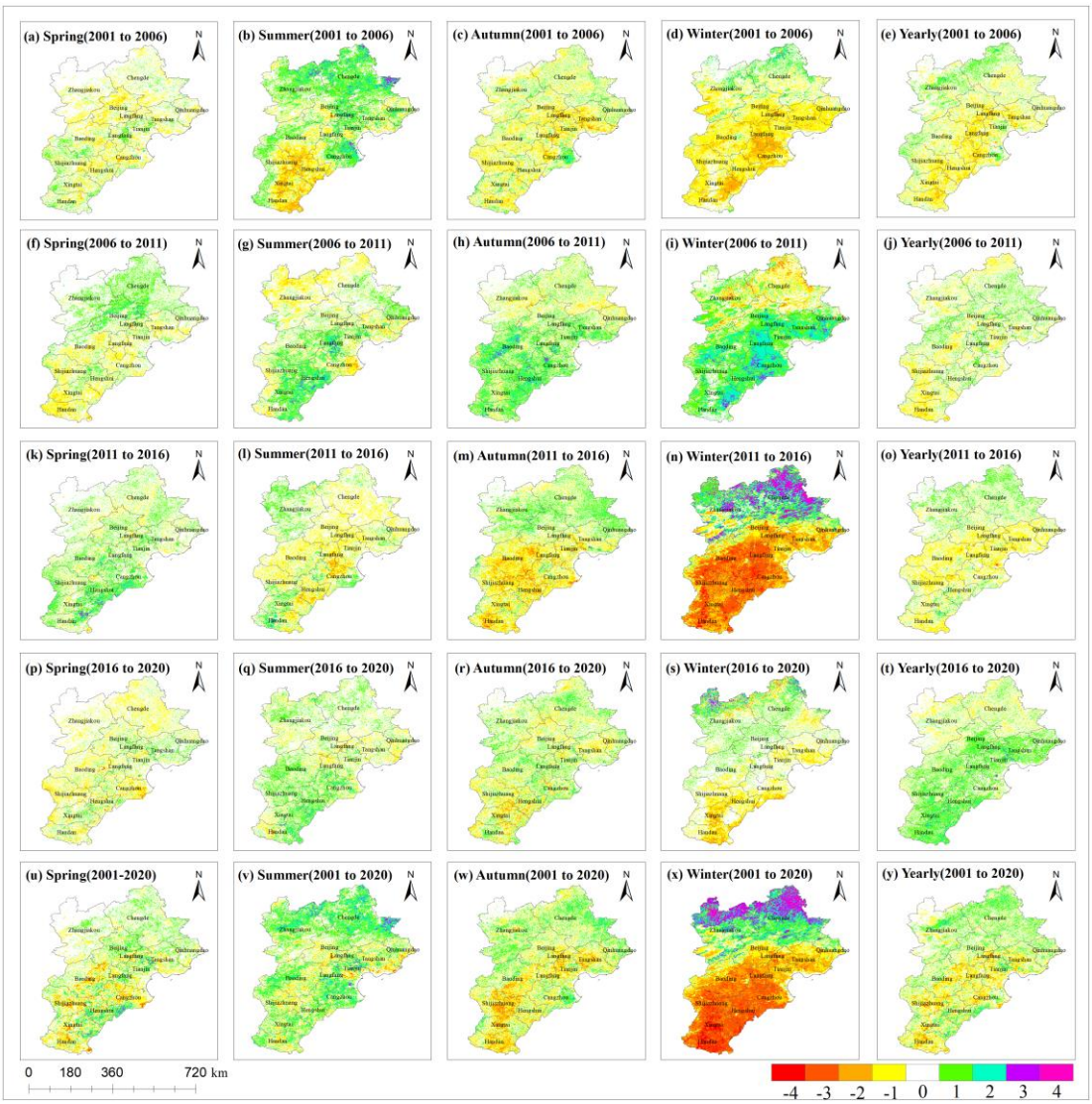

Fig. 6. Spatial-temporal distribution of RSEI change scores.

3.3 Spatial autocorrelation analysis of EEQ

In order to explore whether the spatial adjacent of RSEI has a certain correlation, we plotted the Moran' I scatter plots for summer in 2001, 2006, 2011, 2016, and 2020 shown in Fig. 7. The first and third quadrants are where the scatter points are most concentrated, and the Moran' I values are 0.909, 0.898, 0.917, 0.921, and 0.892, indicating that the spatial correlation of EEQ is strong positive. In other words, the spatial distribution of EEQ showed a characteristic of clustering.

The spatial clustering is shown in Fig. 8 in which the H-H clustering area in the northeast like Chengde, while L-L clustering is in the northwest in these years. From 2001 to 2016, the L-L clustering continuously increased in the south of this study area like Shijiazhuang, Xingtai, and Handan. Besides, the L-L clustering area gradually expanded in Cangzhou and Langfang from 2001 to 2020. The distribution of Not insignificant regions was scattered, and the L-H and H-L regions were almost absent.

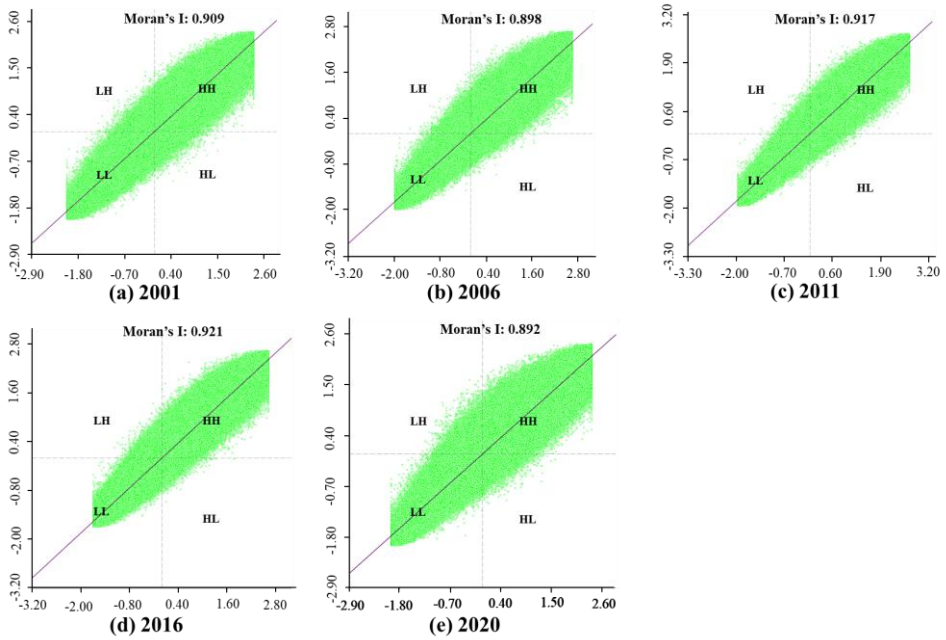

Fig. 7. Moran'I plots distribution of RSEI in summer of 2001, 2006, 2011, 2016, and 2020.

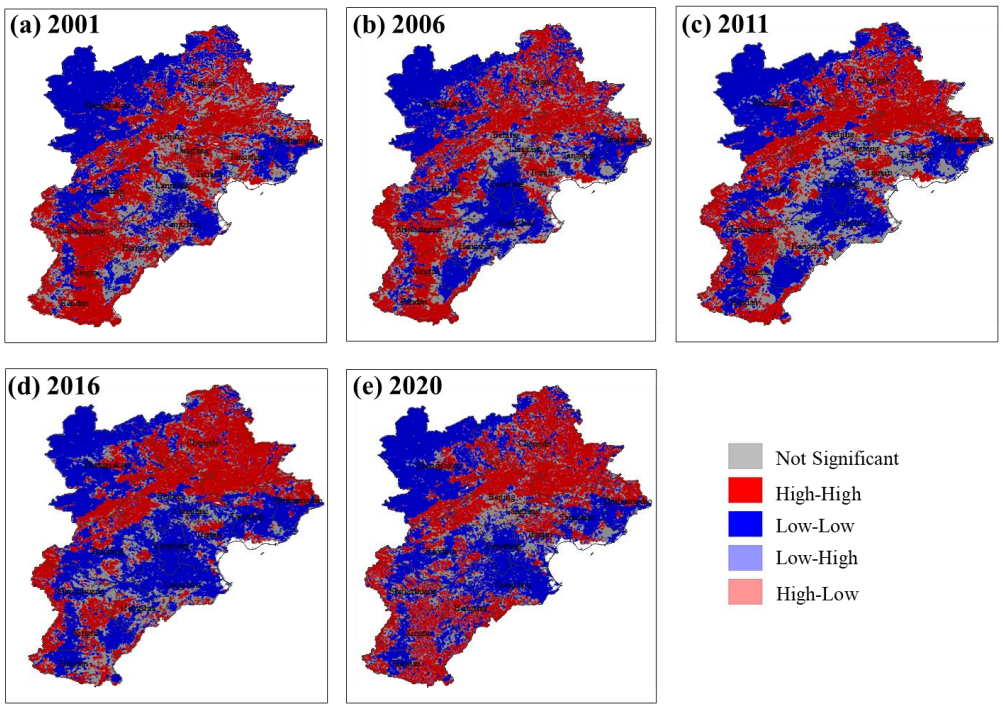

Fig. 8. LISA maps of RSEI in summer of 2001, 2006, 2011, 2016, and 2020.

4. Discussion

The existing studies mainly utilized the same period images in different years to construct the RSEI to assess the temporal and spatial variation of EEQ (Gou and Zhao, 2020; Ji et al., 2020b; Yuan et al., 2021), which mainly considered the inter-annual variation of EEQ in a specific period. However, there is no explanation for why images from a specific time period were used to construct the RSEI to evaluate the EEQ. We synthesized seasonal images to construct RSEI to evaluate EEQ in the JJJ region in this study, which not only considered the interannual variation of EEQ in the same season, but also explored the stability of EEQ in the same season under long-term time series.

The results revealed that the characteristics of the four indicators were primarily concentrated on the PC1, particularly in the summer. Besides, the greenness (NDVI) and wetness (WET) indicators of PC1 had positive effects on EEQ, while heat (LST) and dryness (NDBSI) indicators were negative, respectively (Table. 2). The proved results were similar to the previous researches (Huang et al., 2021; Ji et al., 2022; Yuan et al., 2021).

However, the Pearson correlation coefficient between seasonal RSEI and the four indicators showed a great difference in different seasons (Table. 4). Seasonal RSEI was positively correlated with NDVI and WET, but negatively with NDBSI. Meanwhile, the correlation between LST and RSEI was sometimes positive or negative. Furthermore, previous studies on RSEI time series have typically used a specific period to assess the changing characteristics of RSEI. Instance, some researchers chose the image of the growing season (July to September, 1 June to 31 October, and May to October) to construct RSEI (Cao et al., 2022; Ji et al., 2020b; Jian et al., 2022). But there is no explanation for chose the images of the above period. Fortunately, the correlation signs between the four indicators and summer RSEI showed consistency in different years (NDVI, WET are positive, and LST, NDBSI are negative). All the correlation coefficients in summer showed moderate correlation (abs: 0.4 - 0.6), strong correlation (abs: 0.6 - 0.8), and high correlation (abs: 0.8 - 1) (Table. 4). This can be explained by that vegetation greenness is a key factor for RSEI (Xu and Deng, 2022), and vegetation grows the most flourish and greenest in summer, while the leaves turn yellow in autumn and fall off in spring winter. In addition, to explore the correlation between the four indicators and RSEI in different seasons, we plotted the standard deviation and the mean of the correlation coefficients in different seasons from 2001 to 2020 (Fig. 9). The results showed that the standard deviation of the correlation between the four indicators and RSEI fluctuated slightly in summer, which the std of NDVI, WET, LST, and, NDBSI were 0.005, 0.052, 0.026, and 0.017, respectively.

Table 4

Pearson correlation analysis of seasonal RSEI with four indicators.

Years	Indicators	Spring/ρ	Summer/ρ	Autumn/ρ	Winter/ρ
2001	NDVI	0.884**	**0.941****	0.834**	0.161**
	WET	0.826**	**0.755****	0.824**	0.416**
	LST	-0.415**	**-0.842****	-0.027**	0.873**
	NDBSI	-0.917**	**-0.962****	-0.913**	-0.767**
2006	NDVI	0.853**	**0.953****	0.837**	0.284**
	WET	0.798**	**0.677****	0.826**	0.445**
	LST	0.180**	**-0.854****	-0.218**	0.790**
	NDBSI	-0.953**	**-0.952****	-0.890**	-0.751**
2011	NDVI	0.897**	**0.949****	0.859**	0.0667**
	WET	0.822**	**0.591****	0.779**	0.065**
	LST	-0.171**	**-0.837****	0.032**	0.970**
	NDBSI	-0.890**	**-0.941****	-0.944**	-0.498**
2016	NDVI	0.919**	**0.950****	0.880**	0.386**
	WET	0.832**	**0.665****	0.799**	0.787**
	LST	-0.046**	**-0.842****	-0.358**	-0.718**
	NDBSI	-0.936**	**-0.953****	-0.817**	-0.581**
2020	NDVI	0.922**	**0.941****	0.871**	0.250**
	WET	0.852**	**0.656****	0.841**	0.765**

	LST	-0.046**	**-0.780****	-0.131**	-0.886**
	NDBSI	-0.933**	**-0.914****	-0.856**	-0.254**

Note: ** denotes at level 0.01 (double-tailed), with significant correlation

However, the changes intensities of RSEI of different levels in the same season of adjacent years were relatively slightly (the scores are mainly -1, 0 and 1) (Fig. 6). Land use types, climate change, and human intervention may all be closely related to this (Yuan et al., 2021). Therefore, the spatiotemporal distribution of different levels of RSEI was significantly different in seasons (Fig. 5).

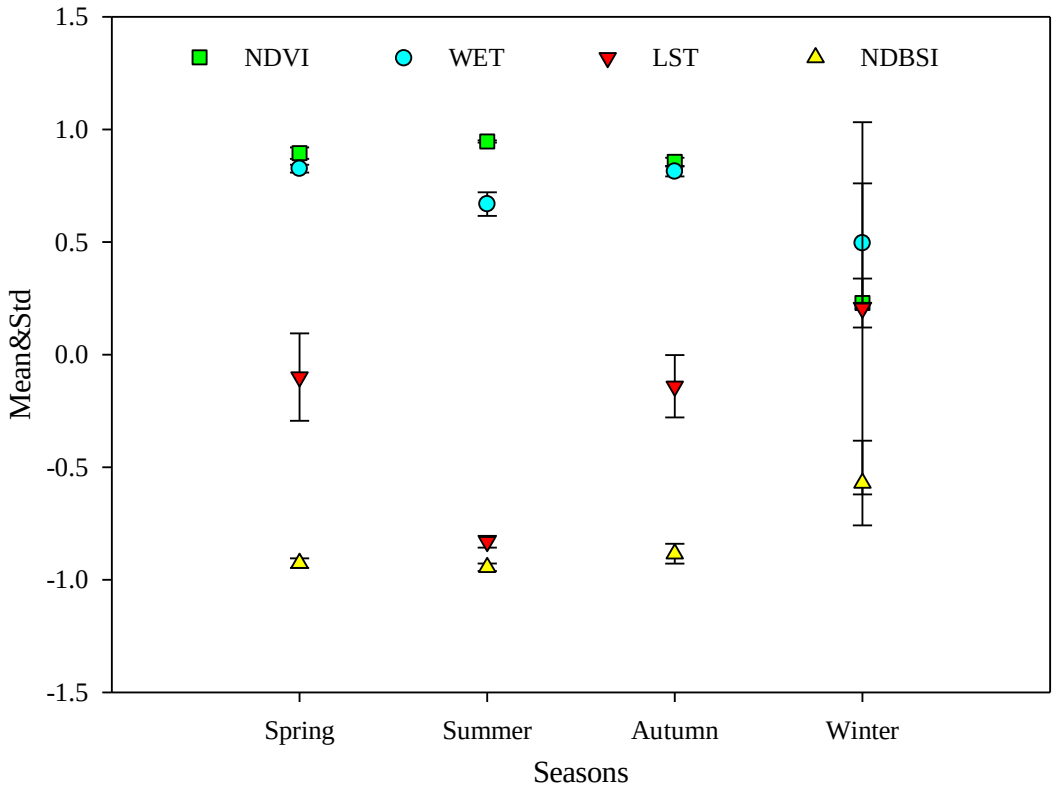

Fig. 9. The mean and standard deviation of correlation coefficients between RSEI and the four indicators in different seasons.

In order to determine the optimal season to construct RSEI for ecological quality assessment, we used VCF to compare with RSEI of different seasons. The percent tree cover showed a consistent spatial distribution in the JJJ region from 2001 to 2020, and the VCF from the western edge to the central region and the northeast (Chengde City) is significantly higher than other regions (Fig. 10). By comparing the spatial distribution changes of the four seasonal RSEI and VCF under the long time series, we found that the spatial distribution of RSEI was consistent with that of VCF only summer. (see Fig. 5). The distribution of RSEI and VCF in the other three seasons showed great differences. Moreover, previous studies have shown that the improvement of ecological environment quality is related to the increase of vegetation cover, and the destruction of vegetation cover will lead to a rapid decline in ecological quality(Cheng and He, 2019; Su et al., 2022).

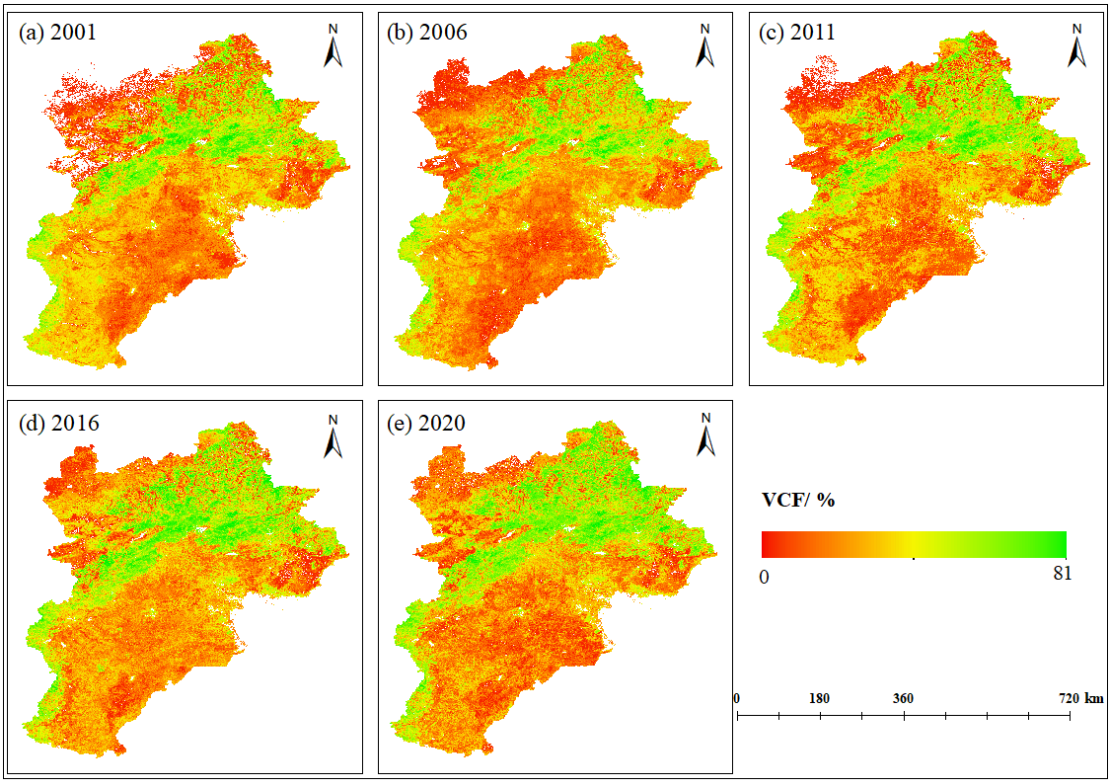

Fig. 10. The spatial distribution of Vegetation Continuous Fields (VCF) of JJJ region from 2001 to 2020.

4.1. Limitation

Although this study analyzed the stability of seasonal RSEI in a long time series and reveals the spatio-temporal variation of seasonal EEQ of the JJJ region and proved that the summer is the most suitable time to conduct RSEI, it has several limitations.1) the traditional RSEI was employed that integrated by NDVI, WET, LST, and NDBSI indicators to assess the changes of EEQ in the JJJ metropolitan region in this study. However, on the basis of the traditional four indicators, some researchers add the factors such as GDP, population, and aerosol optical depth to conduct the MRSEI (Nong et al., 2021; Zhang et al., 2023). 2) We chose MODIS and its product data to calculate RSEI due to the large-scale study area and the long time series study period, but the fine temporospatial changes of EEQ of the coarse-resolution of 500m are difficult to capture. However, the acquisition of the high-precision and multi–temporal used for EEQ analysis is time–consuming and labour–intensive(Huang et al., 2021). Therefore, how to improve the computing power and use multi-temporal and high spatial resolution images (such as Landsat and Sentinel-2) to evaluate EEQ changes in large-scale research areas is an important direction to be studied in the future. 3) The study focuses on the temporospatial evolution of seasonal RSEI. The vast majority bad observations in northern Zhangjiakou and Chengde City despite the synthesis of 3-month images in winter (Fig. 3). Although we employed linear interpolation method for compensate the bad observations, the interpolation results are still abnormal due to the lack of good observation for three months or longer for the pixels (Fig. 6n, 6x). In the reconstruction of long-term continuous missing values in Landsat NDVI time series, the Gap Filling and Savitzky-Golay (GF-SG) method performed best (Chen et al., 2021b), which can be used to reconstruct the bad observations in future research. 4) Chen et al.

(2021a) adopted different synthesis methods (median, max, min, mean) to synthesize the images of the rubber forest disaster before and after the tornado, and proved that the images synthesized by different synthesis methods in different periods have significant differences. In this study, the median function is taken for seasonal image synthesis and constructed RSEI to assess the EEQ of the JJJ region. The influence by using mean, max, or min functions for seasonal image synthesis for RSEI needs further study.

5. Conclusions

Since the RSEI is completely based on remote sensing, the weights of each index are objectively determined from the load values generated by the principal component transformation, and there is no artificial subjective weighting, it is proved that the model has strong robustness. The results showed that the eigenvalues contribution rate of PC1 was more than 71% in the summer, while the other seasons ranged from 40.157% to 60.707%. In addition, the fluctuation of RSEI in the summer from 2001 to 2020 was 0.428, 0.480, 0.505, 0.481, and 0.590, respectively, which indicated that the EEQ of the JJJ has improved in this period. The EEQ in the northeast of the study area was much better than that in other places in the summer, which is consistent with the spatial distribution of VCF. There were significant disparities in the changes of EEQ in the JJJ region across different seasons. Furthermore, the change intensities were relatively low, focusing primarily on the scores -1, 0, and 1. LULC and climate change may explain the variation of EEQ in the JJJ region. RSEI was significantly correlated with the other four indicators and was relatively stable in summer. The findings of this study suggest that the summer images should be employed as much as possible when evaluate the EEQ of urban agglomeration to ensure the veracity of the calculation results of RSEI and the objectivity of ecological quality assessment.

CRediT authorship contribution statement

Shaodong Huang: contributed ideas and designed the study, collected the remote sensing data including the MODIS and its product data, built the algorithm based on GEE, conducted the data analysis, and wrote the manuscript, which all above done with support from the help of all the other authors and all authors gave final approval for publication. **Yujie Li:** data analysis and mapping. **Haowen Hu:** data collected and export to local. **Pengcheng Xue:** data analysis and produced tables. **Nina Xiong:** contributed ideas, designed the study, and wrote the manuscript. **Jia Wang:** contributed ideas, designed the study, conducted the data analysis, and wrote the manuscript with the help of all the other authors.

Declaration of competing interest

The authors declare that they have no known competing financial interests or personal relationships that could have appeared to influence the work reported in this paper.

Acknowledgments

This work was supported by the Fundamental Research Funds for the Beijing Natural Science Foundation Program (grant number 8222069, 8222052); the Natural Science Foundation of China (grant numbers 42071342, 42101473, 42171329), and thank the editors and anonymous reviewers for their kindly view and constructive suggestions.

References

Ahlgren, P., Jarneving, B. and Rousseau, R., 2003. Requirements for a cocitation similarity measure, with special reference to Pearson's correlation coefficient. Journal of the American Society for Information Science and Technology, 54(6): 550-560.

Airiken, M., Zhang, F., Chan, N.W. and Kung, H.T., 2022. Assessment of spatial and temporal ecological environment quality under land use change of urban agglomeration in the North Slope of Tianshan, China. Environ Sci Pollut Res Int, 29(8): 12282-12299.

Anselin, L., 1995. Local indicators of spatial association—LISA. Geographical analysis, 27(2): 93-115.

Cao, J., Wu, E., Wu, S., Fan, R., Xu, L., Ning, K., Li, Y., Lu, R., Xu, X. and Zhang, J., 2022. Spatiotemporal Dynamics of Ecological Condition in Qinghai-Tibet Plateau Based on Remotely Sensed Ecological Index. Remote Sensing, 14(17): 4234.

Chen, B., Yun, T., An, F. and Kou, W., 2021a. Asessment of tornado disaster in rubber plantation in western Hainan using Landsat and Sentinel-2 time series images. National Remote Sensing Bulletin, 25(3): 816-829 (in Chinese).

Chen, Y., Cao, R., Chen, J., Liu, L. and Matsushita, B., 2021b. A practical approach to reconstruct high-quality Landsat NDVI time-series data by gap filling and the Savitzky–Golay filter. ISPRS Journal of Photogrammetry and Remote Sensing, 180: 174-190.

Cheng, Z. and He, Q., 2019. Remote Sensing Evaluation of the Ecological Environment of Su-Xi-Chang City Group based on Remote Sensing Ecological Index (RSEI). Remote Sensing Technology and Application, 34(3): 531-539 (in Chinese).

Deng, Y., Ling, Z., Sun, N. and LV, J., 2021. Daily Estimation of Soil Moisture over Beijing-Tianjin-Hebei Region based on General Regression Neural Network Model. Journal of Geo-information Science, 23(04): 749-761 (In Chinese).

Gao, P., Kasimu, A., Zhao, Y., Lin, B., Chai, J., Ruzi, T. and Zhao, H., 2020. Evaluation of the Temporal and Spatial Changes of Ecological Quality in the Hami Oasis Based on RSEI. Sustainability, 12(18): 7716.

Gong, J., Xie, Y., Zhao, C. and Gao, Y., 2014. Landscape ecological risk assessment and spatial and temporal differentiation of Bailong River Basin in Gansu Province. China Environ. Sci, 34: 2153-2160.

Gorelick, N., Hancher, M., Dixon, M., Ilyushchenko, S., Thau, D. and Moore, R., 2017. Google Earth Engine: Planetary-scale geospatial analysis for everyone. Remote sensing of Environment, 202: 18-27.

Gou, R. and Zhao, J., 2020. Eco-Environmental Quality Monitoring in Beijing, China, Using an RSEI-Based Approach Combined With Random Forest Algorithms. IEEE Access, 8: 196657-196666.

Han, N., Hu, K., Yu, M., Jia, P. and Zhang, Y., 2022. Incorporating Ecological Constraints into the Simulations of Tropical Urban Growth Boundaries: A Case Study of Sanya City on Hainan Island, China. Applied Sciences, 12(13): 6409.

Hang, X., Luo, X., Cao, Y. and Li, Y., 2020. Ecological quality assessment and the impact of urbanization based on RSEI model for Nanjing, Jiangsu Province, China. Ying Yong Sheng tai xue bao= The Journal of Applied Ecology, 31(1): 219-229.

Hu, X. and Xu, H., 2018. A new remote sensing index for assessing the spatial heterogeneity in urban ecological quality: A case from Fuzhou City, China. Ecological Indicators, 89: 11-21.

Huang, H., Chen, W., Zhang, Y., Qiao, L. and Du, Y., 2021. Analysis of ecological quality in Lhasa Metropolitan Area during 1990–2017 based on remote sensing and Google Earth Engine

platform. Journal of Geographical Sciences, 31(2): 265-280.
Hui, J., Bai, Z. and Ye, B., 2021. Eco-Environment Evaluation of Grassland Based on Remote Sensing Ecological Index: A Case in Hulunbuir Area, China. Journal of Computer and Communications, 9(6): 203-213.
Jeong, A. and Dorn, R.I., 2019. Soil erosion from urbanization processes in the Sonoran Desert, Arizona, USA. Land Degradation & Development, 30(2): 226-238.
Ji, J., Tang, Z., Zhang, W., Liu, W., Jin, B., Xi, X., Wang, F., Zhang, R., Guo, B., Xu, Z., Shifaw, E., Xiong, Y., Wang, J., Xu, S. and Wang, Z., 2022. Spatiotemporal and Multiscale Analysis of the Coupling Coordination Degree between Economic Development Equality and Eco-Environmental Quality in China from 2001 to 2020. Remote Sensing, 14(3): 737.
Ji, J., Wang, S., Zhou, Y., Liu, W. and Wang, L., 2020a. Spatiotemporal Change and Landscape Pattern Variation of Eco-Environmental Quality in Jing-Jin-Ji Urban Agglomeration From 2001 to 2015. IEEE Access, 8: 125534-125548.
Ji, J., Wang, S., Zhou, Y., Liu, W. and Wang, L., 2020b. Studying the Eco-Environmental Quality Variations of Jing-Jin-Ji Urban Agglomeration and Its Driving Factors in Different Ecosystem Service Regions From 2001 to 2015. IEEE Access, 8: 154940-154952.
Ji, J., Wang, S., Zhou, Y., Liu, W. and Wang, L., 2021. Studying the coupling coordination degree between socio-economic and eco-environment of Jing-Jin-Ji urban agglomeration during 2001-2015. IOP Conference Series: Earth and Environmental Science, 675(1): 012043.
Jian, K., Wang, S., Wu, X. and Zhang, Q., 2022. Analysis of the Eco-environmental Quality Index in the Tropical Rainforest National Park in China during 1990-2020.
Jing, Y., Zhang, F., He, Y., Kung, H.-t., Johnson, V.C. and Arikena, M., 2020. Assessment of spatial and temporal variation of ecological environment quality in Ebinur Lake Wetland National Nature Reserve, Xinjiang, China. Ecological Indicators, 110: 105874.
Kalantari, Z., Ferreira, C.S.S., Walsh, R.P.D., Ferreira, A.J.D. and Destouni, G., 2017. Urbanization development under climate change: Hydrological responses in a peri-urban Mediterranean catchment. Land degradation & development, 28(7): 2207-2221.
Levin, N., Kyba, C.C., Zhang, Q., de Miguel, A.S., Román, M.O., Li, X., Portnov, B.A., Molthan, A.L., Jechow, A. and Miller, S.D., 2020. Remote sensing of night lights: A review and an outlook for the future. Remote Sensing of Environment, 237: 111443.
Li, Y., Chen, M. and Fu, Y., 2022. Analysis of the changes in the Beijing-Tianjin-Hebei urban agglomeration's spatial structure using NPP-VIIRS data. Bulletin of Surveying and Mapping(02): 50-55 (in Chinese).
Liang, Y., Zou, B., Feng, H. and Liu, N., 2022. Seasonal deviation correction enhanced BGIM downscaling algorithm for remote sensing AOD products. National Remote Sensing Bulletin, 26(08): 1602-1613 (in Chinese).
Liao, W. and Jiang, W., 2020. Evaluation of the Spatiotemporal Variations in the Eco-environmental Quality in China Based on the Remote Sensing Ecological Index, Remote Sensing.
Liao, W., Jiang, W. and Huang, Z., 2022. Spatiotemporal variations of eco-environment in the Guangxi Beibu Gulf Economic Zone based on remote sensing ecological index and granular computing. Journal of Geographical Sciences, 32(9): 1813-1830.
Liu, C., Yang, M., Hou, Y., Zhao, Y. and Xue, X., 2021. Spatiotemporal evolution of island ecological quality under different urban densities: A comparative analysis of Xiamen and Kinmen Islands, southeast China. Ecological Indicators, 124: 107438.

Liu, X.Y., Zhang, X.X., He, Y.R. and Luan, H.J., 2020. Monitoring and Assessment of Ecological Change in Coastal Cities Based on Rsei. The International Archives of the Photogrammetry, Remote Sensing and Spatial Information Sciences, XLII-3/W10: 461-470.

Lobser, S. and Cohen, W., 2007. MODIS tasselled cap: land cover characteristics expressed through transformed MODIS data. International Journal of Remote Sensing, 28(22): 5079-5101.

Maity, S., Das, S., Pattanayak, J.M., Bera, B. and Shit, P.K., 2022. Assessment of ecological environment quality in Kolkata urban agglomeration, India. Urban Ecosystems: 1-18.

McDonald, R.I., Marcotullio, P.J. and Güneralp, B., 2013. Urbanization and global trends in biodiversity and ecosystem services, Urbanization, biodiversity and ecosystem services: Challenges and opportunities. Springer, Dordrecht, pp. 31-52.

Mutanga, O. and Kumar, L., 2019. Google earth engine applications. MDPI, pp. 591.

Nong, L., WANG, J. and YU, Y., 2021. Research on Ecological Environment Quality in Central Yunnan Based on MRSEI Model. Journal of Ecology and Rural Environment, 37(8): 972-982 (in Chinese).

Rousel, J., Haas, R., Schell, J. and Deering, D., 1973. Monitoring vegetation systems in the great plains with ERTS, Proceedings of the Third Earth Resources Technology Satellite—1 Symposium; NASA SP-351, pp. 309-317.

Schneider, A., Mertes, C.M., Tatem, A., Tan, B., Sulla-Menashe, D., Graves, S., Patel, N., Horton, J.A., Gaughan, A. and Rollo, J.T., 2015. A new urban landscape in East–Southeast Asia, 2000–2010. Environmental Research Letters, 10(3): 034002.

Stöckli, R., Vermote, E., Saleous, N., Simmon, R. and Herring, D., 2005. The Blue Marble Next Generation-A true color earth dataset including seasonal dynamics from MODIS. Published by the NASA Earth Observatory.

Su, S., Zhaoning, G., Wenjing, Z., Yuan, Z. and Yifei, W., 2022. Change of vegetation coverage and assessment of ecological environment quality in Beiyun River Basin. Acta Scientiae Circumstantiae, 42(1): 19-27 (in Chinese).

Sun, C., Li, X., Zhang, W. and Li, X., 2020. Evolution of ecological security in the tableland region of the Chinese loess plateau using a remote-sensing-based index. Sustainability, 12(8): 3489.

Tamiminia, H., Salehi, B., Mahdianpari, M., Quackenbush, L., Adeli, S. and Brisco, B., 2020. Google Earth Engine for geo-big data applications: A meta-analysis and systematic review. ISPRS Journal of Photogrammetry and Remote Sensing, 164: 152-170.

Tian, Y., Zhou, D. and Jiang, G., 2020. Conflict or Coordination? Multiscale assessment of the spatio-temporal coupling relationship between urbanization and ecosystem services: The case of the Jingjinji Region, China. Ecological Indicators, 117: 106543.

Turner, W., Spector, S., Gardiner, N., Fladeland, M., Sterling, E. and Steininger, M., 2003. Remote sensing for biodiversity science and conservation. Trends in ecology & evolution, 18(6): 306-314.

Vermote, E., Kotchenova, S. and Ray, J., 2011. MODIS surface reflectance user's guide. MODIS Land Surface Reflectance Science Computing Facility, version, 1: 1-40.

Wan, Z., Hook, S. and Hulley, G., 2015. MOD11A2 MODIS/Terra land surface temperature/emissivity8-day L3 global 1 km SIN grid V006; distributed by NASA EOSDIS LP DAAC. USGS, Sioux Falls.

Wang, H., Jia, G., Fu, C., Feng, J., Zhao, T. and Ma, Z., 2010. Deriving maximal light use efficiency from coordinated flux measurements and satellite data for regional gross primary production

modeling. Remote Sensing of Environment, 114(10): 2248-2258.
Wang, J., Xiao, X., Qin, Y., Dong, J., Geissler, G., Zhang, G., Cejda, N., Alikhani, B. and Doughty, R.B., 2017. Mapping the dynamics of eastern redcedar encroachment into grasslands during 1984–2010 through PALSAR and time series Landsat images. Remote Sensing of Environment, 190: 233-246.
Wang, S., Zhang, X., Zhu, T., Yang, W. and Zhao, J., 2016. Assessment of ecological environment quality in the Changbai Mountain Nature Reserve based on remote sensing technology. Progress in Geography, 35(10): 1269.
Wen, L., Dong, S., Li, Y., Li, X., Shi, J., Wang, Y., Liu, D. and Ma, Y., 2013. Effect of degradation intensity on grassland ecosystem services in the alpine region of Qinghai-Tibetan Plateau, China. PloS one, 8(3): e58432.
Wu, T., Sang, S., Wang, S., Yang, Y. and Li, M., 2020. Remote sensing assessment and spatiotemporal variations analysis of ecological carrying capacity in the Aral Sea Basin. Sci Total Environ, 735: 139562.
Xia, Q., Chen, Y., Zhang, X. and Ding, J., 2022. Spatiotemporal Changes in Ecological Quality and Its Associated Driving Factors in Central Asia. Remote Sensing, 14(14): 3500.
Xiong, Y., Xu, W., Lu, N., Huang, S., Wu, C., Wang, L., Dai, F. and Kou, W., 2021. Assessment of spatial–temporal changes of ecological environment quality based on RSEI and GEE: A case study in Erhai Lake Basin, Yunnan province, China. Ecological Indicators, 125: 107518.
Xu, H., 2013. A remote sensing index for assessment of regional ecological changes. China Environmental Science, 33(5): 889-897 (in Chinese).
Xu, H. and Deng, W., 2022. Rationality Analysis of MRSEI and Its Difference with RSEI. Remote Sensing Technology and Application, 37(01): 1-7 (in Chinese).
Xu, H., Wang, M., Shi, T., Guan, H., Fang, C. and Lin, Z., 2018. Prediction of ecological effects of potential population and impervious surface increases using a remote sensing based ecological index (RSEI). Ecological Indicators, 93: 730-740.
Xu, H., Wang, Y., Guan, H., Shi, T. and Hu, X., 2019. Detecting Ecological Changes with a Remote Sensing Based Ecological Index (RSEI) Produced Time Series and Change Vector Analysis. Remote Sensing, 11(20): 2345.
Yang, X., Meng, F., Fu, P., Wang, Y. and Liu, Y., 2022. Time-frequency optimization of RSEI: A case study of Yangtze River Basin. Ecological Indicators, 141: 109080.
Yang, X., Meng, F., Fu, P., Zhang, Y. and Liu, Y., 2021. Spatiotemporal change and driving factors of the Eco-Environment quality in the Yangtze River Basin from 2001 to 2019. Ecological Indicators, 131: 108214.
Yuan, B., Fu, L., Zou, Y., Zhang, S., Chen, X., Li, F., Deng, Z. and Xie, Y., 2021. Spatiotemporal change detection of ecological quality and the associated affecting factors in Dongting Lake Basin, based on RSEI. Journal of Cleaner Production, 302: 126995.
Yue, H., Liu, Y., Li, Y. and Lu, Y., 2019. Eco-environmental quality assessment in China's 35 major cities based on remote sensing ecological index. Ieee Access, 7: 51295-51311.
Zang, S., Wu, C., Liu, H. and Na, X., 2011. Impact of urbanization on natural ecosystem service values: a comparative study. Environmental monitoring and assessment, 179(1): 575-588.
Zhang, C.-L., Li, Q., Shen, Y.-P., Zhou, N., Wang, X.-S., Li, J. and Jia, W.-R., 2018. Monitoring of aeolian desertification on the Qinghai-Tibet Plateau from the 1970s to 2015 using Landsat images. Science of The Total Environment, 619-620: 1648-1659.

624 Zhang, J., YANG, L., Gong, E., Yu, W., Ren, J. and Liu, M., 2023. Dynamic monitoring of eco-
625 environment quality in Xi' an based on GEE and adjusted RSEI. Acta Ecologica
626 Sinica(05): 1-14 (in Chinese).
627 Zhang, P., Liu, S., Zhao, Z., Liu, C., Xu, L. and Gao, X., 2021a. Supply and demand measurement and
628 spatio-temporal evolution of ecosystem services in Beijing-Tianjin-Hebie Region. Acta
629 Ecologica Sinica, 41(09): 3354-3367 (in Chinese).
630 Zhang, Q., Sun, C., Chen, Y., Chen, W., Xiang, Y., Li, J. and Liu, Y., 2022. Recent Oasis Dynamics and
631 Ecological Security in the Tarim River Basin, Central Asia. Sustainability, 14(6): 3372.
632 Zhang, T., Yang, R., Yang, Y., Li, L. and Chen, L., 2021b. Assessing the Urban Eco-Environmental
633 Quality by the Remote-Sensing Ecological Index: Application to Tianjin, North China. ISPRS
634 International Journal of Geo-Information, 10(7): 475.
635 Zhou, D., Tian, Y. and Jiang, G., 2018. Spatio-temporal investigation of the interactive relationship
636 between urbanization and ecosystem services: Case study of the Jingjinji urban agglomeration,
637 China. Ecological Indicators, 95: 152-164.
638 Zhou, J. and Liu, W., 2022. Monitoring and Evaluation of Eco-Environment Quality Based on Remote
639 Sensing-Based Ecological Index (RSEI) in Taihu Lake Basin, China. Sustainability, 14(9): 5642.
640 Zhu, D., Chen, T., Zhen, N. and Niu, R., 2020. Monitoring the effects of open-pit mining on the eco-
641 environment using a moving window-based remote sensing ecological index. Environmental
642 Science and Pollution Research, 27(13): 15716-15728.
643 Zhu, Z. and Woodcock, C.E., 2012. Object-based cloud and cloud shadow detection in Landsat imagery.
644 Remote Sensing of Environment, 118: 83-94.
645